Electronic structure of Si(100)2×1-Cl studied with angle-resolved photoemission

L. S. O. Johansson* and R. I. G. Uhrberg
Department of Physics and Measurement Technology, Linköping Institute of Technology, S-581 83 Linköping, Sweden

R. Lindsay, P. L. Wincott, and G. Thornton
Interdisciplinary Research Centre for Surface Science and Department of Chemistry, University of Manchester, Manchester M13 9PL, United Kingdom

(Received 11 June 1990)

The chlorine-chemisorbed Si(100)2×1-Cl surface has been studied with polarization-dependent angle-resolved photoemission, employing single-domain surfaces obtained from vicinal Si(100) samples. Contributions from seven Cl-induced surface-state bands are identified in the photoemission spectra in the energy range 5.1–9.4 eV below the Fermi level. One band, at about −8.2 eV initial energy, is attributed to Si—Cl bonding orbitals of mainly p_z character, while four of the higher-energy bands are associated with Cl nonbonding orbitals of mainly p_x, p_y character. A very weak structure at about −9.4 eV initial energy is attributed to Si(s)-Cl(p_z) bonding states. The polarization dependence of the five upper bands in the $\bar{\Gamma}$-$\bar{J}$ and $\bar{\Gamma}$-$\bar{J}'$ directions of the surface Brillouin zone indicates mirror-plane symmetries consistent with a symmetric dimer model.

I. INTRODUCTION

Chlorine adsorption on semiconductor surfaces is of fundamental interest in relation to adsorbate-substrate bonding and adsorbate-induced surface reconstructions. In this regard chlorine has emerged as a prototype halogen adsorbate. An interest also derives from the use of chlorine as a dry etching agent. Consequently, adsorption of chlorine on Si(111) surfaces has been studied extensively,[1–4] both theoretically and experimentally, and Si(111)-Cl has become a prototypical chemisorption system. In contrast, much less is known about the Cl-chemisorbed Si(100) surface. This is surprising considering the extensive studies of other adsorbates, such as hydrogen on Si(100) (see Ref. 5 for a review). Cl on Si(100) has previously been studied with photoemission,[6] electron-energy-loss spectroscopy,[3] surface extended and near-edge x-ray-absorption fine-structure (SEXAFS and NEXAFS) spectroscopies,[7] and thermal desorption.[8]

In early photoemission studies,[6,9] it was shown that the Cl atoms form covalent bonds with the Si surface atoms on Si(111), and it was asserted that the same conclusion is valid for Cl adsorption on Si(100)2×1.[6] On Si(100), the 2×1 periodicity is maintained up to saturation coverage of Cl, suggesting that the Cl atoms bond to Si dimer atoms without breaking the dimer bonds.[6] The expected atomic geometry for the surface, illustrated in Fig. 1(a), is then very similar to the geometry of the well-studied hydrogen-chemisorbed Si(100)2×1-H surface.[5] The electronic structure should also have some similarities, but major differences are expected due to the additional electrons in Cl 3p orbitals on the 2×1-Cl surface.

In the present work, we have studied the Si(100)2×1-Cl surface with polarization-dependent angle-resolved photoelectron spectroscopy (ARPES), using synchrotron light of two different photon energies, 25 eV and 33 eV. ARPES studies of Si(100)2×1 surfaces are normally com-

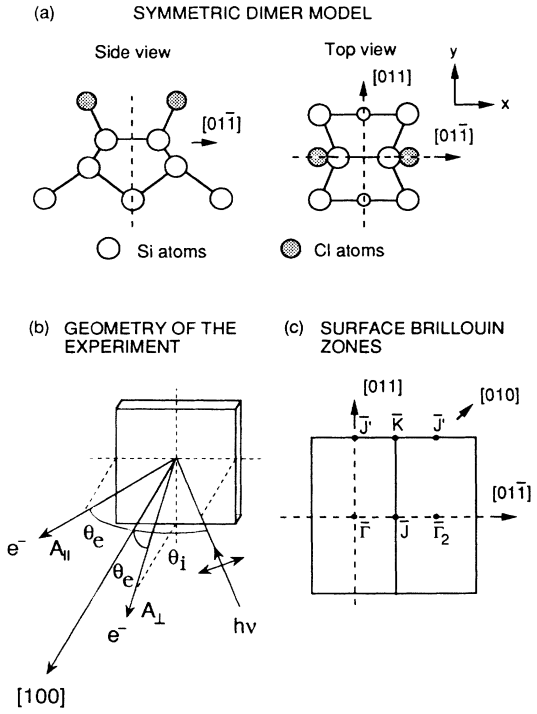

FIG. 1. (a) The symmetric dimer model for the Si(100)2×1-Cl surface. (b) Illustration of the experimental geometries. The photon incidence plane is confined to the horizontal plane. Electrons emitted in the horizontal plane then correspond to the $A_\parallel$ geometry, while electrons emitted in the vertical plane correspond to $A_\perp$. Rotating the sample by 90° around the surface normal allows electronic states along a given direction to be probed with both the $A_\parallel$ and the $A_\perp$ geometries. (c) The surface Brillouin zones of the single-domain surface in the repeated zone scheme. The high-symmetry points are indicated and mirror planes for the symmetric dimer model are marked by dashed lines.

plicated by the presence of two domains, lying perpendicular to each other on the surface. In this work, single-domain Si(100)2×1 surfaces were obtained by using samples cut 4° off the (100) plane towards the [011] direction. After careful annealing of these vicinal samples, terraces separated by double atomic-layer steps are formed, resulting in a single-domain surface.[10] The two-dimensional band structure of the chlorine-induced surface states has been mapped along high-symmetry lines, and the symmetry properties of the surface states have been studied by making use of polarization selection rules.[11] The results are discussed in terms of the 2×1 surface dimer model, where Cl atoms saturate the dangling bonds of the Si dimer atoms.

II. EXPERIMENTAL DETAILS

The ARPES experiments were performed using station 6.2 at the Synchrotron Radiation Source, Daresbury Laboratory. This station employs a toroidal grating monochromator and a Vacuum Generators ADES 400 spectrometer, in which the electron-energy analyzer can be rotated in both the horizontal and vertical planes. The base pressure during the experiments was $\sim 2\times 10^{-10}$ mbar. The ARPES spectra presented here were recorded with an analyzer angular resolution of ±2° and a total energy resolution of ~0.23 eV. A Physical Electronics double-pass cylindrical mirror analyzer was used for Auger-electron spectroscopy (AES) and Si 2*p* core-level photoemission measurements. The Fermi-level (E_F) position was located by recording photoemission spectra from the tantalum sample holder.

The samples were n^+-doped, mirror-polished Si single crystals (arsenic, $\rho = 4$–6 mΩ cm, Wacker-Chemitronic), cut 4° off the (100) plane towards the [011] direction. Before insertion into the vacuum chamber, the samples were cleaned using the etching procedure of Ishizaka and Shiraki.[12] In ultrahigh vacuum the samples were thoroughly outgassed at ~600 °C and then cleaned by stepwise heating up to ~850 °C. A single-domain 2×1 low-energy electron diffraction (LEED) pattern was obtained after a few 1-min anneals at ~850 °C. The formation of regularly spaced double-layer steps was indicated by the characteristic splitting of the LEED spots, as described by Kaplan.[10] The cleanliness of the surface was judged by AES and by noting the intensity of the contamination-sensitive surface states on the clean Si(100)2×1 surface. Only trace amounts of carbon were found in the AES spectrum and no evidence of contamination was observed in the ARPES spectra.

The clean surface was exposed to chlorine gas by dissociating AgCl in an electrochemical cell.[13] The sample was cleaned by annealing just prior to exposure and was maintained at ~200 °C during the exposure to ensure that weakly bound chloride phases were not formed on the surface.[8] Two different samples were prepared in this way, with a good reproducibility of the ARPES spectra. AES was used to check that saturation coverage had been achieved by measuring the peak-to-peak ratio of the Cl *LMM* and Si *LMM* Auger peaks. The resulting ratios indicate close to monolayer Cl coverage of our (100) samples. While this is consistent with the work of Rowe *et al.*,[6] it differs from the saturation coverage of 25% gauged in later work.[3] The origin of this discrepancy is not known. No obvious degradation of the single-domain LEED patterns was observed on Cl adsorption, suggesting that the 2×1 surface reconstruction is not significantly modified by the adsorbate.

The band-gap position of the Fermi level was studied using Si 2*p* core-level photoemission. On the 2×1-Cl surface, it was found that the Fermi level was shifted by 0.5 eV towards the conduction-band minimum, compared to the clean surface. Since the Fermi level at the clean surface is positioned 0.6 eV above the valence-band maximum (E_V) for n^+-doped samples,[14] this indicates that E_F is very close to the conduction-band minimum on the 2×1-Cl surface and that Cl adsorption removes the band bending present on the clean surface. A work function of 5.1 eV for the 2×1-Cl surface was determined by measuring the low-energy cutoff of the ARPES spectra.

In order to explore the polarization dependence of the surface-state emission, ARPES spectra were recorded in the three different geometries shown schematically in Fig. 1(b). At normal (or 18° off-normal) photon incidence, the polarization vector was either *in* the plane defined by the [100] direction and the emission direction, or close to *perpendicular* to the same plane. These will be referred to as the $A_\parallel$ and the $A_\perp$ geometries, respectively. The third geometry employed a higher angle of incidence ($\theta_i = 45°$), the polarization vector of the light being held in the plane containing the [100] direction and the emission direction (as for the $A_\parallel$ case). All the angles of incidence (θ_i) and emission (θ_e) given in this article refer to the [100] direction and *not* to the macroscopic surface-normal. When considering the polarization-dependent data it is important to note that the photon beam is ~70% plane polarized[15] and that a few percent of the annealed surface will contain dimers which are not oriented parallel to the [01$\bar{1}$] direction.[10]

III. EXPERIMENTAL RESULTS

A selected set of ARPES spectra, recorded with different emission angles and the $A_\parallel$ geometry in the $\bar{\Gamma}$-$\bar{J}'$ direction of the surface Brillouin zone (SBZ), are shown in Fig. 2. The SBZ is illustrated in Fig. 1(c). Three main chlorine-induced structures can be identified in the spectra, denoted S_1, S_2, and S_3, with energies of approximately −8.2, −6.7, and −5.7 eV, respectively. Figure 3 contains a selection of spectra recorded in the same emission direction but in the $A_\perp$ polarization geometry. Three Cl-induced structures are also present in these spectra, with S_4 and S_5 lying at similar energies to the S_2 and S_3 peaks in Fig. 2, but with different relative intensities. In the $A_\parallel$ spectra, S_2 dominates over much of the angular interval, whereas in the $A_\perp$ spectra, S_5 is stronger. In normal emission, the S_2 peak in the $A_\parallel$ spectra is diminished. However, in the $\theta_i = 45°$ geometry S_2 dominates also in normal emission, as illustrated in Fig. 4. In off-normal emission in the $\bar{\Gamma}$-$\bar{J}'$ direction, spectra recorded in the $\theta_i = 45°$ geometry are similar to the

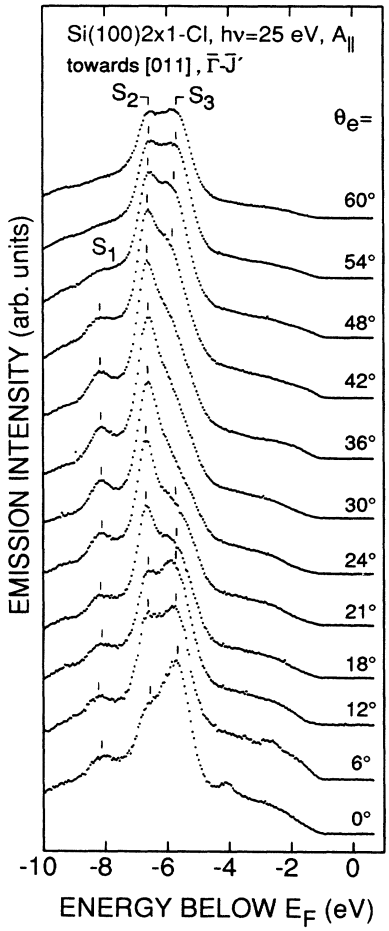

FIG. 2. ARPES spectra for emission in the $(01\bar{1})$ plane, recorded with 25-eV photon energy and the $A_{\parallel}$ geometry. The angle of incidence (θ_i) was 18° for $\theta_e = 0°$, and 6° for $\theta_e = 12°$, and 0° for the remaining spectra.

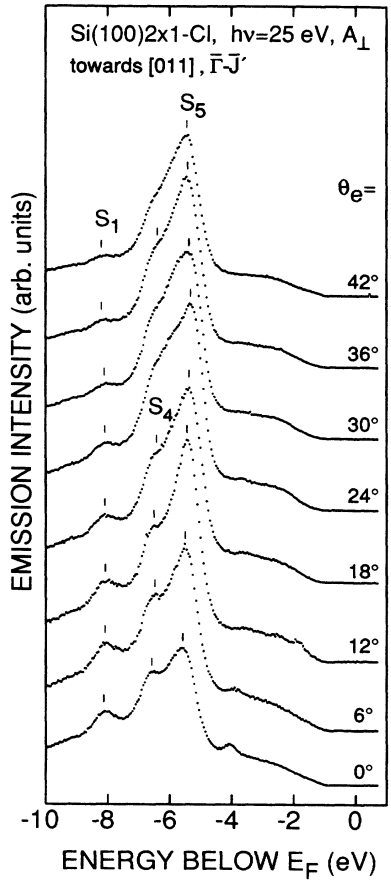

FIG. 3. ARPES spectra for emission in the $(01\bar{1})$ plane, recorded with 25-eV photon energy and the $A_{\perp}$ geometry. The angle of incidence (θ_i) was 18° for all spectra.

corresponding $A_{\parallel}$ spectra. A rather weak peak, labeled S_6, was found near $\bar{\Gamma}$ in the $\theta_i = 45°$ spectra at an energy of about -9.4 eV (see Fig. 4). Another small peak is seen at around -4.1 eV for low-emission angles in Figs. 2 and 3, and is interpreted as a Si bulk feature, based on a comparison with spectra from the clean Si(100)2×1 surface.

The dispersions of the surface states in the $\bar{\Gamma}$-$\bar{J}'$ direction are shown in Fig. 5, along with the projected bulk band structure, calculated using the linearized augmented plane-wave method.[16] In general, the dispersions are quite flat, with a width of 0.2 eV or less. The reason for distinguishing between S_2,S_3 in the $A_{\parallel}$ spectra and S_4,S_5 in the $A_{\perp}$ spectra, respectively, now becomes clear: the dispersions of these structures do not overlap. The energy positions of the strong, dominant peaks in the spectra (solid symbols in Fig. 5) are easily determined, but the energies of the weak peaks and the structures appearing as shoulders (open symbols in Fig. 5) are more uncertain.

The dispersions of the Cl-induced surface states in the

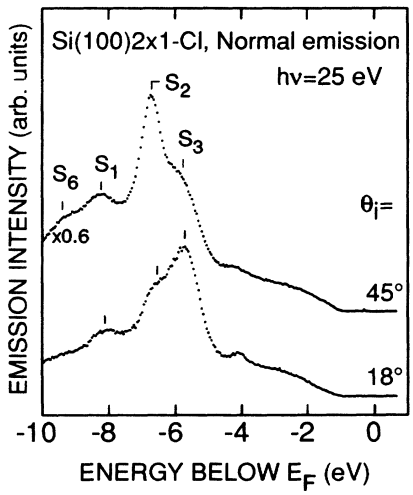

FIG. 4. ARPES spectra recorded at normal emission for two different incidence angles. The light was incident in the $(01\bar{1})$ plane.

$\bar{\Gamma}$-$\bar{J}$ direction are shown in Fig. 6. Samples of the corresponding spectra are contained in Fig. 7, which shows spectra pertaining to $\mathbf{k}_{\parallel}$ points near $\bar{\Gamma}$ in the second SBZ [see Fig. 1(c)]. Most of the dispersions are quite flat along the $\bar{\Gamma}$-$\bar{J}$ direction. Moreover, the dispersions obtained with the $A_{\parallel}$ and $A_{\perp}$ geometries overlap more closely along the $\bar{\Gamma}$-$\bar{J}$ direction and the peaks at around -6.6 and -5.7 eV are labeled $S_{2,4}$ and $S_{3,5}$, respectively. Only for the $S_{3,5}$ peaks near $\bar{J}$ in the second SBZ do we find a small difference between the $A_{\parallel}$ and $A_{\perp}$ dispersions. Near $\bar{\Gamma}$ in the second SBZ, a pronounced shoulder, denoted S_7, appears at around -5.1 eV initial energy, in the $\theta_i = 45°$ geometry. A corresponding structure is not observed at normal emission, or in any other $\bar{\Gamma}$ data.

IV. DISCUSSION

As noted above, the atomic and electronic structure of the Si(100)2×1-Cl surface should be similar to the well-studied hydrogen-chemisorbed Si(100)2×1-H surface. On the 2×1-H surface, two surface-state bands associated with the Si—H bonds were identified in a previous ARPES study.[17] These bands are separated by about 1.0 eV due to the π-bonding interaction within the dimers. The bands have mirror-plane symmetry, consistent with a symmetric dimer model of the surface. Assuming a symmetric dimer model for the 2×1-Cl surface, the Si—Cl bonds should similarly give rise to two surface bands, of mainly mixed Si $3p_z$ and Cl $3p_z$ character. Another four filled surface bands should also be present on a symmetric dimer surface, being associated with the Cl nonbonding orbitals of mainly p_x,p_y character. In Ref. 6, it was proposed that some mixing between the p_z and p_x or p_y orbitals could occur, due to the expected off-normal adsorption geometry. For symmetric dimers, the Cl—Si bond is estimated to be directed $\sim 25°$ off the surface normal.[7] While keeping this in mind, we continue to refer to the

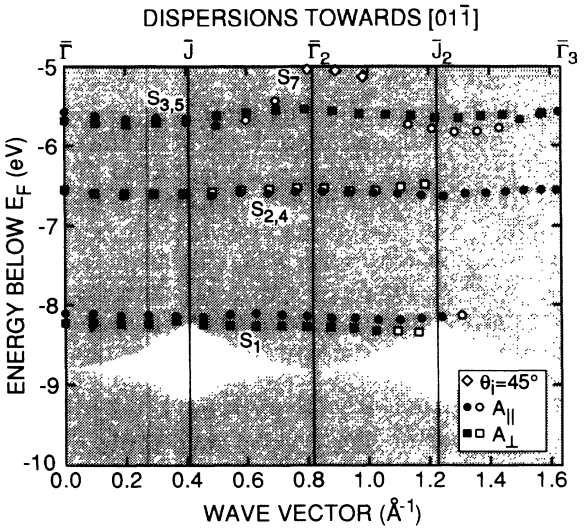

FIG. 6. The empirical dispersions of the Cl-induced surface states in the [01$\bar{1}$] direction. Other details are identical to Fig. 5.

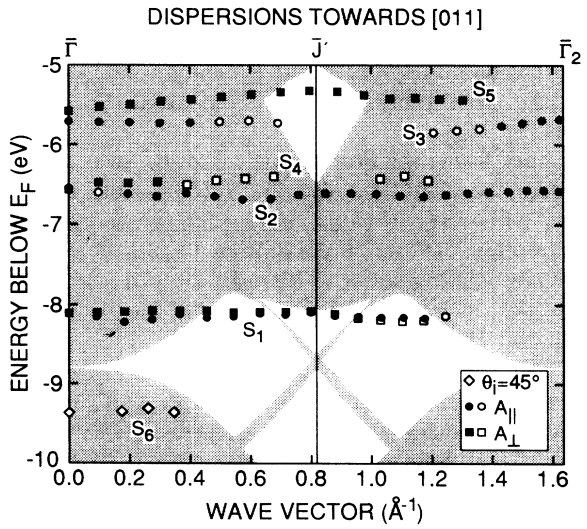

FIG. 5. The empirical dispersions of the Cl-induced surface states in the [011] direction on the single-domain Si(100)2×1-Cl surface, recorded with 25-eV photon energy. The symbols indicate the experimental geometries employed. Data points from spectra recorded with $\theta_i = 45°$ are included where they deviate significantly from the $A_{\parallel}$ points. Open symbols denote shoulders and weak structures in the spectra, for which the energy positions are more uncertain. The shaded region is the projected bulk band structure (Ref. 16). The value $E_F - E_V = 1.1$ eV was used to reference the binding-energy scale.

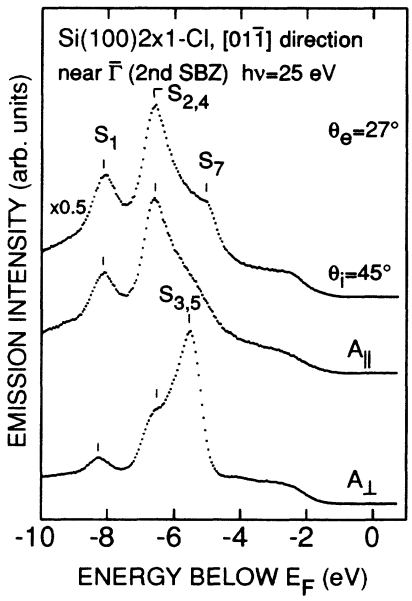

FIG. 7. ARPES spectra recorded in the (011) plane with a photon energy of 25 eV. The emission angle ($\theta_e = 27°$) was chosen in order to examine states near the $\bar{\Gamma}$ point in the second SBZ (along the $\bar{\Gamma}$-$\bar{J}$ line). The experimental geometries are indicated in the figure.

bonding and nonbonding states as having mainly p_z and p_x or p_y character, respectively. With the coordinate system defined in Fig. 1(a), p_x orbitals are directed within the vertical plane containing the dimer bond [the (011) plane], and p_y orbitals are directed perpendicular to this plane. In line with earlier work on Si(100) (Ref. 6) and Si(111) (Refs. 2, 6, 9, and 18) surfaces, it is reasonable to associate S_1 with one or both of the Si-Cl $3p_z$ bands and S_6 with Si $3s$–Cl $3p_z$ states. This leaves four of the S_2, S_3, S_4, S_5 ($S_{2,4}$ and $S_{3,5}$ along the $\bar{\Gamma}$-$\bar{J}$ direction), and S_7 peaks to be assigned to the nonbonding p_x,p_y bands. The possible assignments of these structures are discussed further below.

The symmetry properties of electronic states associated with the symmetric dimer model are described by Appelbaum, Baraff, and Hamann.[19] The model, for which the point group is C_{2v}, has mirror symmetry in the two planes perpendicular to the surface containing [011] and [01$\bar{1}$]; i.e., the (01$\bar{1}$) and (011) planes, respectively. Four irreducible representations exist for this group: A_1 (completely symmetric), B_1 [odd under reflection in the (01$\bar{1}$) mirror plane], B_2 [odd under reflection in the (011) mirror plane], and A_2 (odd under reflection in both mirror planes), using the coordinate system of Ref. 19. For the surface states in the symmetric dimer model, the group of the wave vector at the high-symmetry points in the first SBZ is the full C_{2v} group, with the above-mentioned possible representations. Along the symmetry lines $\bar{\Gamma}$-$\bar{J}'$ and $\bar{\Gamma}$-$\bar{J}$ ([011] and [01$\bar{1}$] directions, respectively), the symmetries of the surface states are reduced to even or odd symmetry with respect to the respective mirror planes which contain these directions. Utilizing this symmetric-dimer picture, within a single dimer the Cl p_x orbitals can be arranged into A_1 (bonding) and B_1 (antibonding) symmetry combinations, and the p_y orbitals into combinations with A_2 (antibonding) and B_2 (bonding) symmetry.

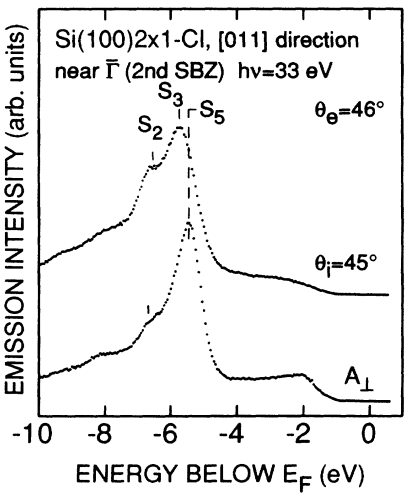

FIG. 8. ARPES spectra, recorded in the (01$\bar{1}$) plane with a photon energy of 33 eV. The emission angle (θ_e=46°) corresponds to $k_\parallel$ points near $\bar{\Gamma}$ in the second SBZ along the $\bar{\Gamma}$-$\bar{J}'$ line.

The selection rules appropriate to mirror-plane photoemission indicate that even initial states are suppressed in the $A_\perp$ geometry and, conversely, emission from odd states is suppressed in the $A_\parallel$ geometry, as well as in the θ_i=45° geometry.[11] The clear polarization dependence of S_2, S_3, S_4, and S_5 along the $\bar{\Gamma}$-$\bar{J}'$ line, *and* $S_{2,4}$, $S_{3,5}$, and S_7 along the $\bar{\Gamma}$-$\bar{J}$ line indicates that mirror-plane selection rules exist on the 2×1-Cl surface consistent with the presence of symmetric dimers [see Fig. 1(a)]. These rules suggest that the states contributing to the S_2 and S_3 peaks along the $\bar{\Gamma}$-$\bar{J}'$ line should have even symmetry and we might then associate these peaks with p_x and p_y bonding combinations. Conversely, the S_4 and S_5 peaks can be associated with odd states (p_x and p_y antibonding combinations) with respect to the (01$\bar{1}$) mirror plane. It may be questioned whether the energy difference between the S_2 and S_4 features is significant; but for the dispersions of S_3 and S_5, on the other hand, there is an obvious difference in energy. This is particularly clear at high emission angles, where both S_3 and S_5 are intense, which is illustrated in Fig. 8. Here the S_3 and S_5 peaks are probed near $\bar{\Gamma}$ in the second SBZ with 33-eV photon energy. The energy separation between the two peaks is ~0.3 eV.

It should also be noted that at normal emission the S_2 peak is suppressed in the $A_\parallel$ geometry, but is strong in the θ_i=45° geometry, as seen in Fig. 4. This can be explained by the higher symmetry of the $\bar{\Gamma}$ point. In normal emission, only electrons from totally symmetric initial states will be emitted by the z component of the polarization vector, and the emission from these states will be suppressed when the polarization vector is parallel to the surface. This indicates that the S_2 peak seen in the $A_\parallel$ geometry and with θ_i=45° corresponds to a surface band that has A_1 symmetry at $\bar{\Gamma}$, which is also consistent with the even symmetry of this peak in both mirror planes.

In the $\bar{\Gamma}$-$\bar{J}$ direction the $S_{2,4}$ peak has an even-symmetry contribution, and the $S_{3,5}$ peak has odd symmetry, with respect to the mirror plane containing the $\bar{\Gamma}$-$\bar{J}$ direction. These are the only two bands in the region of the nonbonding states to be resolved in the $A_\parallel$ and $A_\perp$ geometries, as indicated by the overlap over most of the $\mathbf{k}_\parallel$ interval of the dispersions of $S_{2,4}$ and $S_{3,5}$. This suggests an assignment of $S_{2,4}$ to p_x and $S_{3,5}$ to p_y states, since in the symmetric dimer model both p_x bands should be even and both p_y bands odd with respect to the (011) mirror plane. Since the bonding and the antibonding p_x and p_y bands have the same symmetry, they would not be resolved in our data if their separation were small. Hence, the observation of four separate bands along the $\bar{\Gamma}$-$\bar{J}'$ direction and only two main features along the $\bar{\Gamma}$-$\bar{J}$ direction is consistent with the symmetric dimer model.

On the basis of the interpretation employed above, S_7 remains unassigned. This feature appears at around −5.1 eV initial energy in Γ-$\bar{J}$–direction spectra near $\bar{\Gamma}$ in the second SBZ, and has even symmetry. A large splitting of the Si-Cl mainly p_z bands, arising from an intradimer overlap of Si-Cl p_z orbitals, could provide an explanation for a feature additional to the four Cl $p_{x,y}$ non-

bonding bands. Such an interaction would require a reassignment of the $p_{x,y}$ bands, with S_4 being identified with the antibonding counterpart of S_1, which should have odd symmetry along the $\bar{\Gamma}$-$\bar{J}'$ direction. However, this implies an energy separation between the two p_z bands of ~ 1.5 eV, which is significantly larger than the 1-eV separation of the Si $3p_z$-H $1s$ bands observed for Si(100)2×1-H.[17] The alternative possibility, and that implied in the analysis above, is that the energy splitting of the p_z bands is sufficiently small to prevent the bonding and antibonding components being resolved. This is consistent with the weak polarization dependence of S_1 along the $\bar{\Gamma}$-$\bar{J}'$ direction, where the Si-Cl p_z bands should have opposite symmetry, and the stronger polarization dependence around $\bar{\Gamma}_2$ in the $\bar{\Gamma}$-$\bar{J}$ direction (see Fig. 7), where both bands should be even. Another possible assignment of S_7 would be to Si-Si back-bond states. Si(111)1×1-Cl back-bond states have been identified in a calculated band structure and observed experimentally at energies slightly above the nonbonding Cl states.[18]

V. SUMMARY

The chlorine-chemisorbed Si(100)2×1-Cl surface has been studied with polarization-dependent angle-resolved photoemission from single-domain 2×1-Cl surfaces. Seven Cl-induced structures were identified in the ARPES spectra in the energy range 5.1–9.4 eV below E_F. By comparison with data for chlorine-chemisorbed Si(111)-Cl surfaces, features at around −9.4 and −8.2 eV initial energy can be assigned to bands having Si(s)-Cl(p_z) character and Si-Cl p_z character, respectively. The polarization dependence of the five uppermost states indicates mirror-plane symmetries in the $\bar{\Gamma}$-$\bar{J}$ and $\bar{\Gamma}$-$\bar{J}'$ directions. This is consistent with the symmetry properties expected on the basis of a symmetric dimer model.

Of the five higher-energy structures, four can be associated with the Cl nonbonding orbitals of mainly p_x,p_y character, with a fifth tentatively assigned to a Si-Si back-bond state. However, there is some uncertainty in the interpretation because of the many overlapping spectral features. We conclude, on the basis of the present data, that it is difficult to unambiguously determine the origin of all the Cl-induced structures in the ARPES spectra. To make further progress in this analysis, calculated band structures are needed for comparison with the experimental data.

ACKNOWLEDGMENTS

The authors would like to thank the staff at the Daresbury Laboratory for their help and support and Professor Göran Hansson for stimulating and helpful discussions. This work was supported partly by the Swedish Natural Science Research Council and partly by the United Kingdom Science and Engineering Research Council. One of us (R.L.) would like to thank Harwell Laboratory for financial support.

*Present address: IBM Research Division, Zurich Research Laboratory, CH-8803 Rüschlikon, Switzerland.

[1]For a review, see H. H. Farrell, in *The Chemical Physics of Solid Surfaces and Heterogeneous Catalysis,* edited by D. A. King and D. P. Woodruff (Elsevier, Amsterdam, 1984), Vol. 3B, Chap. 5.

[2]R. D. Schnell, D. Rieger, A. Bogen, F. J. Himpsel, K. Wandelt, and W. Steinman, Phys. Rev. B **32**, 8057 (1985).

[3]N. Aoto, E. Ikawa, and Y. Kurogi, Surf. Sci. **199**, 408 (1988).

[4]R. G. Jones, Prog. Surf. Sci. **27**, 25 (1988), and references therein.

[5]For relevant references, see S. Ciraci, R. Butz, E. M. Oellig, and H. Wagner, Phys. Rev. B **30**, 711 (1984); L. S. O. Johansson, R. I. G. Uhrberg, and G. V. Hansson, Phys. Rev. B **38**, 13490 (1988).

[6]J. E. Rowe, G. Margaritondo, and S. B. Christman, Phys. Rev. B **16**, 1581 (1977).

[7]G. Thornton, P. L. Wincott, R. McGrath, I. T. McGovern, F. M. Quinn, D. Norman, and D. D. Vvedensky, Surf. Sci. **211/212**, 959 (1989).

[8]R. B. Jackman, H. Ebert, and J. S. Foord, Surf. Sci. **176**, 183 (1986).

[9]M. Schlüter, J. E. Rowe, G. Margaritondo, K. M. Ho, and M. L. Cohen, Phys. Rev. Lett. **37**, 1632 (1976).

[10]R. Kaplan, Surf. Sci. **93**, 145 (1980).

[11]J. Hermanson, Solid State Commun. **22**, 9 (1977).

[12]A. Ishizaka and Y. Shiraki, J. Electrochem. Soc. **133**, 666 (1986).

[13]The Cl source is a modified version of the design described in N. D. Spencer, P. J. Goddard, P. W. Davies, M. Kitson, and R. M. Lambert, J. Vac. Sci. Technol. A **1**, 1554 (1983).

[14]The value $E_F - E_{V'} = 0.6$ eV for the clean surface of an n^+-doped crystal is based on the pinning position for the Si(111)7×7 surface [0.63 eV, F. J. Himpsel, G. Hollinger, and R. A. Pollak, Phys. Rev. B **28**, 7014 (1983)] and core-level studies on Si(111)7×7 and Si(100)2×1 [R. I. G. Uhrberg (unpublished)].

[15]D. S.-L. Law (private communication).

[16]For computational details, see P. E. S. Persson, PhD thesis, Linköping University, 1986, dissertation No. 147.

[17]L. S. O. Johansson, R. I. G. Uhrberg, and G. V. Hansson, Phys. Rev. B **38**, 13490 (1988).

[18]P. K. Larsen, N. V. Smith, M. Schlüter, H. H. Farrell, K. M. Ho, and M. L. Cohen, Phys. Rev. B **17**, 2612 (1978).

[19]J. A. Appelbaum, G. A. Baraff, and D. R. Hamann, Phys. Rev. B **14**, 588 (1976).

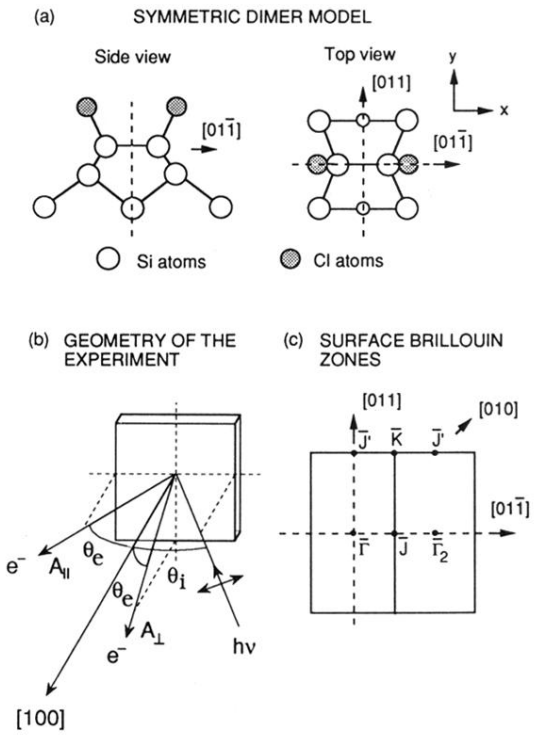

FIG. 1. (a) The symmetric dimer model for the Si(100)2×1-Cl surface. (b) Illustration of the experimental geometries. The photon incidence plane is confined to the horizontal plane. Electrons emitted in the horizontal plane then correspond to the $A_{\parallel}$ geometry, while electrons emitted in the vertical plane correspond to $A_{\perp}$. Rotating the sample by 90° around the surface normal allows electronic states along a given direction to be probed with both the $A_{\parallel}$ and the $A_{\perp}$ geometries. (c) The surface Brillouin zones of the single-domain surface in the repeated zone scheme. The high-symmetry points are indicated and mirror planes for the symmetric dimer model are marked by dashed lines.

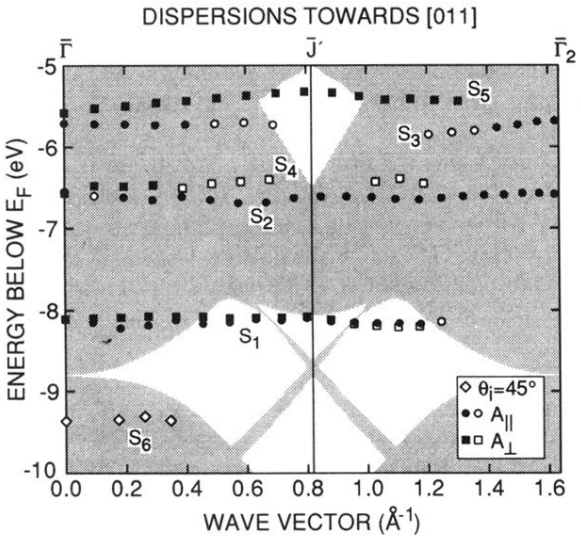

FIG. 5. The empirical dispersions of the Cl-induced surface states in the [011] direction on the single-domain Si(100)2×1-Cl surface, recorded with 25-eV photon energy. The symbols indicate the experimental geometries employed. Data points from spectra recorded with $\theta_i = 45°$ are included where they deviate significantly from the $A_{||}$ points. Open symbols denote shoulders and weak structures in the spectra, for which the energy positions are more uncertain. The shaded region is the projected bulk band structure (Ref. 16). The value $E_F - E_V = 1.1$ eV was used to reference the binding-energy scale.

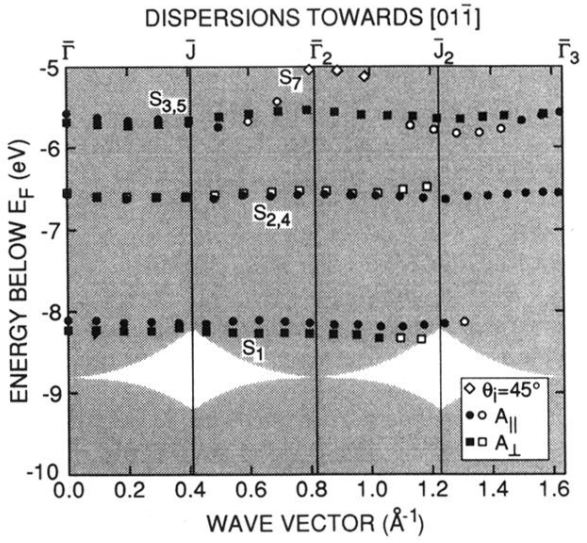

FIG. 6. The empirical dispersions of the Cl-induced surface states in the [01$\bar{1}$] direction. Other details are identical to Fig. 5.